A Platform for Free-Weight Exercise Monitoring with Passive Tags

Han Ding, *Student Member, IEEE*, Jinsong Han, *Senior Member, IEEE*, Longfei Shangguan, *Student Member, IEEE*, Wei Xi, *Member, IEEE*, Zhiping Jiang, *Student Member, IEEE*, Zheng Yang, *Member, IEEE*, Zimu Zhou, *Student Member, IEEE*, Panlong Yang, *Member, IEEE*, and Jizhong Zhao, *Member, IEEE*

Abstract—Regular free-weight exercise helps to strengthen natural movements and stabilize muscles that are important to strength, balance, and posture of human beings. Prior works have exploited wearable sensors or RF signal changes for activity sensing, recognition, and counting, etc.. However, none of them have incorporated three key factors necessary for a practical free-weight exercise monitoring system: recognizing free-weight activities on site, assessing their qualities, and providing useful feedbacks to the bodybuilder promptly. Our FEMO system provides an integrated free-weight exercise monitoring service that incorporates all the essential functionalities mentioned above. FEMO achieves this by attaching passive RFID tags on the dumbbells and leveraging the Doppler shift profile of the reflected backscatter signals for on-site free-weight activity recognition and assessment. The rationale behind FEMO is 1) since each free-weight activity owns unique arm motions, the corresponding Doppler shift profile should be distinguishable to each other. 2) Doppler profile of each activity has a strong spatial-temporal correlation that implicitly reflects the quality of the activity. We implement FEMO with COTS RFID devices and conduct a two-week experiment. The preliminary result from 15 volunteers demonstrates that FEMO can be applied to a variety of free-weight activities, and provide valuable feedbacks for activity alignment.

Index Terms—Activity recognition and assessment, RFID

1 Introduction

Free-weight exercise is indispensable in a balanced exercise program and provides numerous health benefits. It helps to stabilize bones and muscles that are relevant to strength, balance and posture, and contributes to weight loss and overall health [1]. Some researches recommend free-weight training twice a week for adults [2], even for those who walk or run regularly. Moreover, some individuals may prefer free-weight exercises to aerobic exercises as the main fitness activities simply for lifestyle or convenience reasons.

Monitoring and evaluation supports are crucial for free-weight exercises. Compared with aerobic exercises, e.g., running, people are more vulnerable to inefficient training or even accidental injuries in free-weight training. Stretching or warping muscles improperly, e.g., to the wrong direction or at a high speed, can lead to strains and tears. Timely guidance is also important for exercise safety and quality since people might forget their progress, skip essential steps, or miscount a sequence.

Despite academic and commercial success in aerobic exercise monitoring [4], [5], [6], [7], [8], there is a void in automatic free-weight exercise monitoring and evaluation. A personal coach is still by far the most common solution to free-weight training monitoring, which incurs high recruitment costs [9]. Unlike aerobic exercises where speed, distance and terrain are essential, the quality of free-weight training is mostly defined by repetitions, durations and activity sets. Existing schemes on general activity recognition [10], [11] and aerobic exercise tracking [6], [7] fail to capture such high-fidelity information for free-weight exercises. Some pioneer work explored inertial sensors, e.g., accelerometer and gyroscope, for free-weight training monitoring [12], [13], yet these techniques cannot reliably handle the variety of arm motion patterns and diverse training paces. Furthermore, they also require body-worn sensors to function, which poses inconvenience and might cause unwanted motion changes during training. A promising alternative is to leverage wireless signals for device-free activity sensing. Recent research has explored the feasibility of WiFi signals for gesture and activity recognition [14], [15], [16], yet either involves customized hardware (e.g., software radios [15]) or targets at location-aware activities [16], thus unsuitable for ubiquitous free-weight exercise tracking.

In this paper, we design FEMO, an automatic, non-invasive and light-weight Free-weight Exercise MOnitoring system. We enable non-invasive free-weight exercise monitoring by attaching passive Radio Frequency IDentification (RFID) tags on assisted instruments (e.g., dumbbells) during training, and analyzing signals backscattered from tags during exercises. Attaching passive RFID tags on instruments like a dumbbell poses minimum overhead due to their negligible weight and

- *H. Ding, J. Han, W. Xi, Z. Jiang, and J. Zhao are with the School of Electronic and Information Engineering, Xi'an Jiaotong University, Xian, Shi 710049, China. E-mail: {dinghanxjtu, jiangzp.cs}@gmail.com, {hanjinsong, xiwei, zjz}@mail.xjtu.edu.cn.*
- *L. Shangguan is with the Department of Computer Science, Princeton University, Princeton, NJ 08544. E-mail: longfeis@cs.princeton.edu.*
- *Z. Yang is with the School of Software and TNList, Tsinghua University, Beijing, Shi 100084, China. E-mail: hmilyyz@gmail.com.*
- *Z. Zhou is with the Computer Engineering and Networks Laboratory, ETH Zurich, Zürich 8092, Switzerland. E-mail: zzhou@tik.ee.ethz.ch.*
- *P. Yang is with the College of Communications Engineering, PLA University of Science and Technology, Nanjing 210007, China. E-mail: panlongyang@gmail.com.*

Manuscript received 1 Feb. 2016; revised 12 Feb. 2017; accepted 22 Mar. 2017. Date of publication 6 Apr. 2017; date of current version 1 Nov. 2017.
For information on obtaining reprints of this article, please send e-mail to: reprints@ieee.org, and reference the Digital Object Identifier below.
Digital Object Identifier no. 10.1109/TMC.2017.2691705

size. FEMO works by analyzing the Doppler shifts extracted from the backscattered signals. It automatically recognizes, counts, and assesses the exercises on-site and in real time. The detailed assessment feedbacks are also displayed on FEMO's UI module to assist activity rectification.

The design of FEMO involves the following challenges:

(1) *How to detect and extract accurate Doppler shifts from backscatter signals?* Doppler shifts are accessible from commercial RFID readers via a standard API. However, the raw Doppler measurements are too noisy to precisely portray the tag movements (i.e., dumbbell trails).

We address this problem by transforming the received phases from backscatter signals into the corresponding Doppler shifts (Section 3.1). FEMO tracks this Doppler stream and segments the Doppler shifts of each activity performed even at diverse paces (Section 3.2).

(2) *How to recognize free-weight exercises on-site?* Traditional activity recognition schemes rely on sophisticated feature selection and complex classification techniques for accurate recognition, which incur a large computational latency and are sensitive to training data.

FEMO addresses this problem by analyzing the temporal patterns of RF signals affected by body movements. Our observation is that each free-weight activity is a unique combination of basic arm motions. These combined arm motions exhibit unique yet stable Doppler shift profiles in the temporal domain, producing light-weight and robust features for activity recognition. We detail this idea and optimize the recognition process in Section 3.3.

(3) *How to assess user performances?* Since FEMO aims to provide useful feedbacks to users as guidance for improper activity rectification, it is important to quantify the quality of each performed activity.

In FEMO, we define a set of metrics evaluating the quality of activities during free-weight exercises from both the local and global views. An assessment framework is proposed to evaluate both the activity details and the activity consistency within each training group.

We implement FEMO as a framework consisting of four core modules: Doppler value pre-processing, activity segmentation, activity recognition and activity assessment. We prototype FEMO on commodity hardware including a Commercial Off-The-Shelf (COTS) RFID reader, a directional antenna, and two passive RFID tags attached to the dumbbells. It runs on a central server and processes the tag reading stream in pipeline. It also provides an interface to other applications such as activity counting and training process tracker, where they can obtain the current activity primitives from FEMO via programming interfaces. We evaluate the performance of FEMO on free-weight training data collected in two weeks from 15 volunteers. The data cover 1,534 minutes of exercises, with 4,500 repetitions of 10 representative exercises. Results demonstrate that FEMO can be applied to various representative free-weight activities, and provide valuable feedbacks to users, especially beginners.

We summarize the contributions of this paper as follows:

- We introduce the first passive RFID-based system for free-weight exercise monitoring. This system enables on-site activity recognition and assessment, and provides rich feedbacks to the user for activity rectification. Different from prior works that only coarsely recognize to which type the activity is belonging, our FEMO system can provide fine-grained measurements on the activity by using the subtle Doppler values retrieved from COTS passive RFID devices.
- We present a set of algorithms to effectively extract free-weight exercise information from backscatter signals. Specifically, our algorithms enable 1) extracting minute Doppler shifting from noisy tag readings reported by commercial RFID readers; 2) segmenting the Doppler streaming such that each segment contains an intact activity; 3) assessing the exercise performance and providing useful feedbacks to the bodybuilder.
- We extend the system to multi-user scenario by using multiple antennas. We address the challenging issues in this extension, including the overlapped monitoring regions, pairing between a tag and antenna, and under-sampling caused by collisions.
- Last but not the least, we establish a proof-of-concept prototype and conduct two-week experiments. Results demonstrate the effectiveness of our system. It can detect ten typical free-weight activities with an average accuracy of 90.4 percent, and facilitate rectifying irregular exercise behaviors, especially for fitness novices.

2 Overview

This section briefly introduces the taxonomy of the targeted free-weight activities and the overall work-flow of FEMO.

2.1 Taxonomy of Free-Weight Activities

In this paper, we focus on ten common and representative free-weight activities, which can train different parts of the muscle groups. We choose these popular activities based on a two-week questionnaire investigation on 50 fitness enthusiasts in our university. Similar to [12], we categorize these activities into different groups based on the muscle groups desired to be trained. Fig. 1 illustrates ten free-weight activities of interests, which will be used to demonstrate our work throughout this paper.

2.2 FEMO Work-Flow

Fig. 2 presents the work-flow of FEMO. It contains four major steps: preprocessing, activity segmenting, activity recognition, and activity assessment.

The first step is preprocessing, where the system purifies the raw phase readings and computes the Doppler shifts. In this step, FEMO first mitigates the noisy phase readings introduced by the hardware heterogeneity of the reader and the inconsistency of tag orientations. FEMO then computes the Doppler values and finally employs a moving-average filter to smooth the Doppler values.

The second step is to segment the Doppler stream, such that each segment contains a single free-weight activity. A main challenge lies in the heterogeneity of Doppler profiles with respect to different activities. We find that the state-of-the-art, e.g., threshold-based filters [4], [12] or peak detection schemes [17], fails to segment the activity precisely. In FEMO, we exploit the stochastic characteristics of Doppler values and design a KL-divergence based segmentation algorithm. This algorithm works efficiently and adapts to various free-weight activities and users.

The third step is to recognize each activity from the Doppler segment. Towards accurate and prompt recognition, we

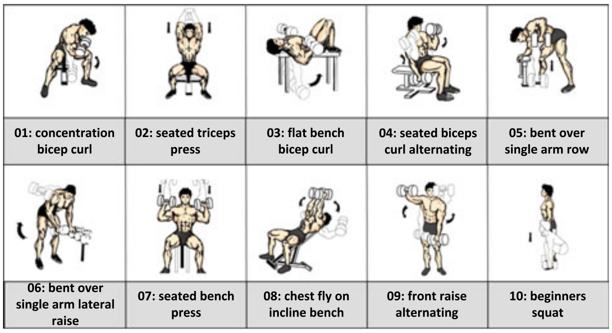

Fig. 1. Sketches of the tested free-weight activities [3].

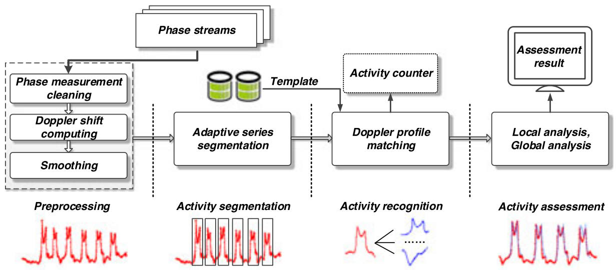

Fig. 2. An overview of FEMO's work-flow.

build up a body movement model and observe that each activity has a unique yet stable combination of arm motion trails. Based on this observation, we employ the Doppler profile as the feature of each activity and design a fingerprint based activity recognition scheme. To improve the recognition efficiency, we leverage the motion order of arms to prune the unqualified matching candidates in advance.

The final step is to measure the quality of each activity and provide valuable feedbacks to users. In FEMO, we assess each activity from both the local and global views. Local analysis concentrates on the activity details by comparing the proposed features against the standard ones. The global analysis focuses on the consistency of each group of activities by measuring the smoothness and continuity of activities within each group. The assessment results are displayed on the end-user interface to assist activity rectification.

3 System Design

This section details the FEMO design and highlights the challenges, key observations, and core techniques behind the activity segmentation, recognition and assessment of FEMO.

3.1 Data Acquisition and Preprocessing

3.1.1 Preprocessing

Phase Measurement Smoothing. Instead of directly using the noisy Doppler shifts from the API, we deduce the Doppler shifts from the phase measurement reported by the commercial reader. To achieve precise Doppler shifts, it is crucial to minimize the phase noise. We change the tag orientation with respect to the antenna with a step of 6 degree and examine how sensitive the phase measurement is to tag orientations. The antenna is set to be 2 m away from the tag. Fig. 3a shows the raw phase measurements when the tag rotates 2π (marked as red points). We find that due to the inherent circuit noise, the phase values fluctuate continuously and randomly. We further test the distribution of these

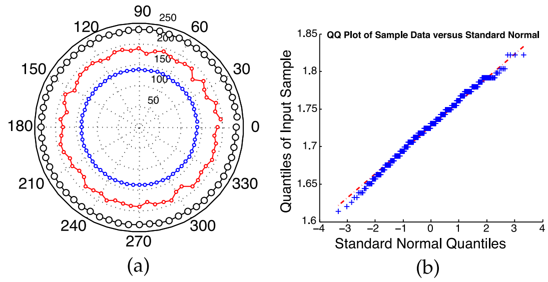

Fig. 3. (a) Phase measurements under different tag orientations. (b) QQ Plot of sample data versus standard normal distribution.

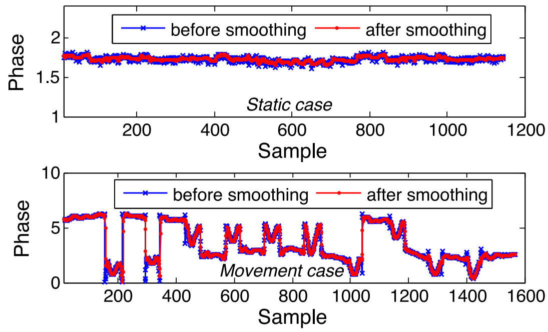

Fig. 4. Phase measurements before/after smoothing under static/movement cases.

measurements against the standard Gaussian distribution (shown in Fig. 3b). The linearity of the points on the Q-Q plot suggests that the data are normally distributed, with a standard deviation of 0.0332 radian. Based on this observation, we model the phase measurement θ as a Gaussian random variable $\mathcal{N}(\mu, 0.0332)$. We then utilize the standard Kalman Filter [18] to smooth the phase values. We test various look-back window sizes, and empirically set it as 10 which optimizes the smoothing performance.

Fig. 4 shows the phase measurement before/after smoothing in both the static and movement cases. The difference indicates that the Kalman filter effectively enhances the stability of phase measurements of static tags. For the moving-tag case, we can see that the phase values change steadily after filtering. Yet they still retain a clear profile of the free-weight activity.

Deducing Doppler Shifts. Doppler shifts are generated due to the relative movement between a transmitter and a receiver, e.g., the stationary reader and the moving tag. Theoretically, to calculate Doppler we should estimate the change in RF frequency. However, the commercial reader does not support this function, i.e., reporting the frequency change. Hence, we adopt a phase-based method to measure the corresponding Doppler. Suppose at time t_i and t_{i+1}, the reader receives two consecutive signals from the moving tag, with the phase readings θ_i and θ_{i+1}. Let v be the tag's moving speed within the period of $[t_i, t_{i+1}]$. v can be regarded as a constant due to the short interval between two consecutive tag readings. Hence the distance (d) that the tag moves equals to $v \cdot (t_{i+1} - t_i)$. On the other hand, we know that the signal in the backscatter communication traverses 2 times of d. Thus we have

$$2v \cdot (t_{i+1} - t_i) = \lambda \cdot \left(\frac{\theta_{i+1} - \theta_i}{2\pi} \right). \tag{1}$$

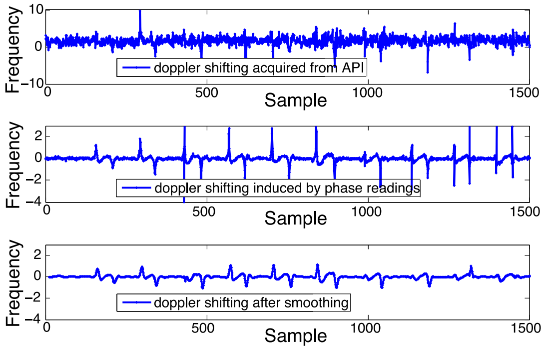

Fig. 5. Doppler shift of 10 consecutive *Bent-over lateral raise*.

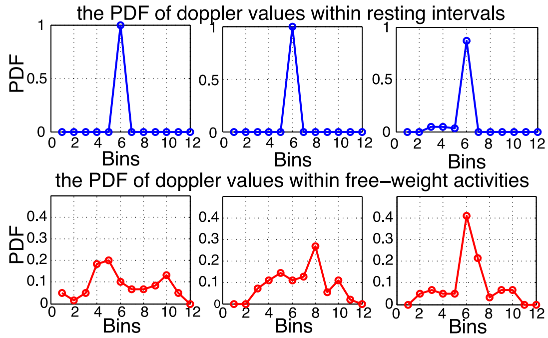

Fig. 6. PDF of doppler values within different windows.

The Doppler shift can be further expressed as [19]

$$f = \frac{v}{\lambda} = \frac{\theta_{i+1} - \theta_i}{4\pi \cdot (t_{i+1} - t_i)}. \tag{2}$$

Fig. 5b shows the phase-deduced Doppler shifts. The measurements are collected when a volunteer performs *Bent-over lateral raise* ten times. Compared with the noisy Doppler values reported by the API (Fig. 5a), the deduced Doppler values clearly show ten repetitive patterns.

Despite the high resolution, from Fig. 5b we find that the deduced doppler value still fluctuates over time. This is because the time interval between any two consecutive readings may vary due to the random access mechanism of ALOHA protocol [20]. Such non-uniform time intervals lead to Doppler fluctuations and jitters that overwhelm the original appearance of each activity. Therefore, after computing the Doppler value, we apply a moving average filter over the last n readings (n=10 in FEMO) to smooth the Doppler values. Fig. 5c shows the final results.

3.2 Activity Segmentation

The activity segmentation module identifies Doppler segments that are likely to contain a complete free-weight activity. We define each segment as $\kappa_i = (t_s : t_e)$, with start time t_s and end time t_e within the Doppler stream. The segmentation yields a set of segments K, with each containing a free-weight activity: $K = \{\kappa_1, \kappa_2, \ldots, \kappa_m\}$.

There has been extensive efforts on activity segmentation [10]. Most of them assume that each activity will exhibit a clear peak in the received signal stream. Thus by comparing each signal strength with a static threshold, the activity segments will be located accordingly. However, such a solution is unsuitable for FEMO as a free-weight activity usually contains multiple peaks within an activity period. The one-peak detection scheme may split one activity into multiple segments.

3.2.1 Key Observations

In FEMO, the activity segmentation scheme is based on the fact that people tend to take a short rest after each activity to control the training pace. We term such a short rest as a *resting interval*. The resting intervals have small Doppler values, which naturally separate the activities. Thus by extracting the start and end times of each resting interval, we can acquire each activity segment accordingly. Our segmentation scheme leverages two insights:

- The sharp Doppler values usually take a small portion of the whole data within the resting interval.
- Except for the sharp Doppler values incurred by the pose adjustment, the remaining Doppler readings within the resting interval are relatively small and stable.

Thus if we split a resting interval into multiple consecutive windows, the distribution of Doppler values within each window should be similar. Conversely, the Doppler values outside the resting interval corresponds to the free-weight activity. These values change rapidly and show a completely different distribution from those in the resting interval.

3.2.2 Segmentation Scheme

The above analysis leads us to an adaptive segmentation scheme based on the KL divergence [21]. Denote the Doppler stream as $S = (s_i) \in \mathbb{R}^{1\times N}$, where N is the number of discrete time points $t_1, \ldots, t_N$ at which the Doppler values are sampled. For each w consecutive Doppler values, we group them into a window. Within each window, we further categorize the Doppler values into multiple bins. The bin size is empirically set as 0.35. Then we can get the discrete probability distribution function (PDF) of Doppler values within each window. Given two consecutive windows w_i and w_j, let P and Q be their PDF, respectively. The KL divergence of Q from P is defined as

$$D_{KL}(P||Q) = \sum_i P(i) \cdot ln \frac{P(i)}{Q(i)}. \tag{3}$$

The KL divergence measures the information loss when Q is used to approximate P. In FEMO, there are three cases:

(1) both windows are within the resting interval;
(2) both windows are within the activity period;
(3) one is within the resting interval and another is within the activity period;

In the first case, $D_{KL}(P||Q)$ will be close to zero due to the similar probability distributions within these two windows (Fig. 6a). In the latter two cases, $D_{KL}(P||Q)$ will be significantly larger than zero as the distribution varies sharply among these two windows (Fig. 6b). Hence by checking $D_{KL}(P||Q)$, we can ascertain whether the current window is within the resting interval or not. After finding all windows within the resting interval, we can extract the activity segment accordingly. Fig. 7 shows the segmentation result over a Doppler stream, we see that all of these ten activities are correctly identified. We also notice the Doppler profile of each activity is completely contained in the corresponding segment, indicating accurate and robust segmentation.

Determining a Proper Window Size. In FEMO, multiple windows will be employed for activity segmentation. The window size, termed as w, should not be determined arbitrarily. On one hand, a large window size may cover extra

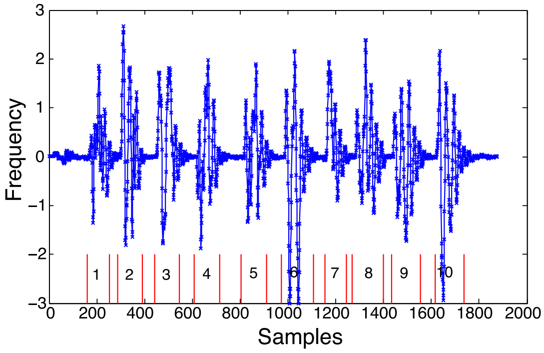

Fig. 7. Segmentation result of 10 activity performing.

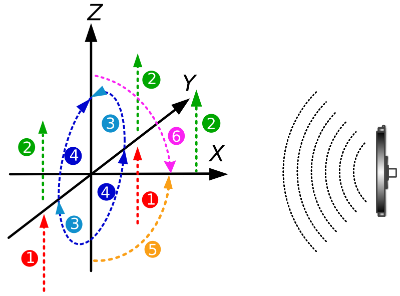

Fig. 8. Trails of six basic arm motions.

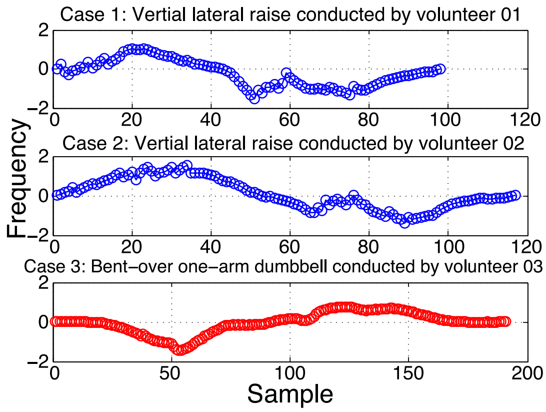

Fig. 9. Doppler profiles of activities.

portions instead of the resting period only, leading to inaccurate segmentation. On the other hand, a small window size tends to generate massive windows, resulting in high computational overhead. In both cases, the segmentation performance of FEMO will be degraded. We thus determine the window size adaptively by using the equation: $\frac{t \cdot r}{d \cdot n}$, where n is the number of tags (which is related to the number of users) within the detection region of the reader's antenna, r is the reading rate of the reader (e.g., r = 340 for ImpinJ R420 reader), t is the minimum duration of the resting interval which is set to 0.5 s empirically, and d is the granularity coefficient. The intuition behind is as follows. Ideally, each tag within the reader's detection region will be interrogated $\frac{r}{n}$ times per second. We can acquire $\frac{t \cdot r}{n}$ Doppler values during the resting interval. To guarantee that each activity can be correctly identified, the resting interval should contain at least 2 windows. Taking the multipath effect into account, we conservatively set $d = 4$. Thus, the window size automatically increases with a small number of tags, yet decreases when the tag population increases. In this way, the window size adapts to the ambient and population change in FEMO.

3.3 Activity Recognition

The activity recognition module aims to identify the free-weight activity within each segment. Many previous works focus on building a robust activity recognition system [4], [12], [15], [16], [22]. The main principle is to extract unique features for the activity from the input signals, and train a classifier to distinguish each unlabelled activity. However, this method has two major drawbacks. First, the system performance is sensitive to the training set. If the training set is small or biased, the classifier will suffer from low recognition accuracy. Although a larger training set may lead to a more accurate classifier, it will incur a higher overhead (e.g., time and cost for collecting the ground-truth) on system realization and deployment. Second, such a method suffers from higher latency. We are motivated to design our activity recognition scheme balancing accuracy and overhead.

3.3.1 Body Model and Key Observation

Activity recognition is directly linked to body movement analysis. We aim to build a robust activity recognition scheme via the body movement patterns. The key intuition behind this scheme is that each free-weight activity can be abstracted to either an *arm stretching motion* or an *arm spinning motion*. For example, the Bent over single arm row (activity 05) stands for stretching the arm vertically, whereas the Chest fly on incline bench (activity 08) refers to the process of spinning both arms 90 degree in parallel. Based on different moving directions, the arm stretching/spinning motions can be further divided into 6 kinds of *basic arm motions* (shown in Fig. 8). By systematically analysing the motion trails of these fundamental arm motions, we have the following observations:

(1) Each arm motion corresponds to a unique motion trail, which yields a unique Doppler pattern.
(2) By correlating the free-weight activity with arm motions, each free-weight activity corresponds to a unique combination of fundamental arm motions, either with different numbers or different orders. For detailed demonstration, we list the combinations of each activity in Fig. 11.

An insight derived from above observations is that the Doppler profile of each free-weight activity is *distinguishable* from each other, leading to *large inter-class variations*. On the other hand, the execution of each activity follows the standard back eight and demonstrates the similar arm motions. Thus, performing an activity multiple times will result in multiple *similar* Doppler profiles, with a *large intra-class similarity* among them. Fig. 9 depicts the Doppler profile of three activities. We can see that the two upper subfigures show the stability of Doppler profiles corresponding to the same activities, while the lowermost confirms that the Doppler profile disperses in case of different free-weight activities. Hence, the Doppler profile can discriminate the free-weight activities and act as a reliable signature.

3.3.2 Fingerprint Matching

FEMO compares the profile in each segment against the standard to identify free-weight activities. Hence we need to evaluate the similarity between two Doppler profiles. We argue that the euclidean-distance metric is unsuitable since

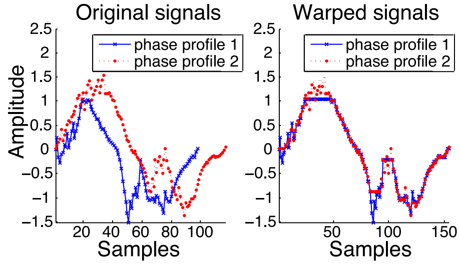

Fig. 10. Original and warped signals.

activity segments may vary in length due to personal preferences, physical characters (weight, height) and other reasons.

FEMO uses *Dynamic Time Warping* (DTW) [23] to compute the similarity between two Doppler profiles. The benefits are twofold. On one hand, DTW compares two profiles with different lengths. On the other hand, DTW automatically compresses or stretches a sequence to minimize the distance between two sequences, thus focusing on the shape similarity rather than the absolute values. Fig. 10 shows the Doppler profiles of bent-over one-arm dumbbell that are aligned with DTW. We observe that Doppler profile 1 is stretched and shifted to match with Doppler profile 2.

Note that in current implementation of FEMO, we only focus on the data of predefined ten activities. Other unknown activities (including picking up, putting down the weights, or walking around, etc..) will be filtered out by comparing their DTW distances with a pre-calibrated threshold in advance.

3.3.3 Hierarchical Activity Recognition Framework

Directly using DTW for activity recognition is costly. The complexity of DTW is $O(mn)$, indicating a large overhead for long Doppler profiles, especially when we have to compare one Doppler profile against all candidates in the database. To reduce the computational overhead, we design a hierarchical activity recognition framework based on two observations on the arm motion pattern:

(1) The free-weight activity involves either a single arm motion or two arm motions.
(2) For the two arm motion activities, they are either conducted in parallel or alternatively.

Fig. 11 shows the decision-tree based recognition scheme. At the first level, FEMO classifies the candidate by detecting whether the current activity is a single arm activity or not. This process can be achieved by checking whether the attached two tags on the dumbbells are detected together. If yes, FEMO further classifies the candidate by checking whether the current two-arm activity is performed alternatively or not. This process can be done by examining the concurrency of activities within these two doppler streams. Specifically, let t_o and t_l be the overlapping duration and the longest time duration of two activity segments, respectively. If $t_o \geq \beta \cdot t_l$, FEMO ascertains these two motions are conducted in parallel. With above pruning process, we can shrink the candidate group to no more than half its original size. In our implementation, we set β as $\frac{2}{3}$ by default. Identifying the tag ID takes $O(1)$ time, while judging the concurrency of two activities is achievable in $O(1)$ time. These two simple operations help to prune the unqualified profiles in an early stage of activity recognition, thereby improving the computational efficiency. After the activity recognition, all activities will be labelled and stored for activity assessment.

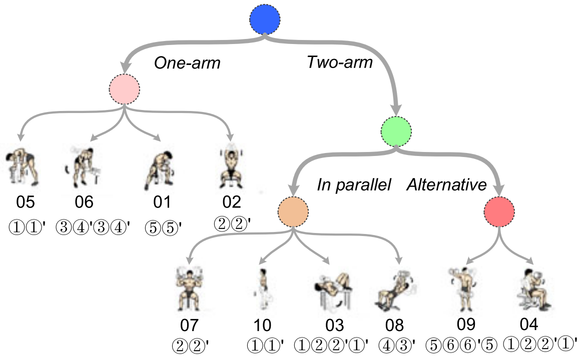

Fig. 11. The pipeline of activity recognition.

3.3.4 Extending to Multi-User Scenarios

Besides recognizing the activity for single-user scenarios, in this section we extend FEMO to multi-user scenarios. It is intuitive to use multiple antennas to deal with multiple users. Each antenna can cover a particular region and monitor one user. However, deploying multiple antennas will raise several challenging issues. First, multiple antennas may have overlapped areas. Each individual tag might be read by more than one antenna, i.e., the tag might be within different monitoring regions of those antennas. Thus, which antenna should be assigned to monitor a certain tag is a problem. In fact, this requires find a proper pairing between a tag and an antenna. Another challenge is under-sampling, which is caused by the TDMA based scheduling strategy of RFID antennas or ALOHA based anti-collision mechanism among multiple tags.

To address above issues, we first analyze the impact of angle between the reader and the tag. Since Doppler will have a projection to the reader-to-tag direction, this angle has a non-trivial impact on the Doppler profile. The slight deformation of Doppler profile might increase the DTW distance between it and the template, resulting in a decrease of the recognition accuracy. Thus, for a given tag we propose to assign the antenna that is directly facing the tag as the desired antenna. The reader we adopted supports up to four antennas, thus FEMO can monitor four users concurrently, i.e., one antenna for each user. In practice, an RFID reader can connect more antennas (e.g., 16) via an antenna hub.

FEMO addresses the multi-user problem with following three steps: determining the pairing between the antenna and the subject, interpolation-assisted Doppler profile construction, and activity recognition.

- *Determining the pairing*. It is possible that all the four antennas can read a subject's tag when he/she is performing the activity. Thus, solving the pairing problem should consider the radiation pattern of RFID antennas. According to the typical radiation pattern of directional patch antenna, the transmitting power radiated at an angle (to the left/right of the beam center) is less than the power in the center of the beam. For example, for the antenna with the gain of 8 dBi (adopted by our current implementation), the power radiated at 36 degrees is 3 dB less than the beam in the center (6 dB for the angle of 60 degrees and 15 dB for the angle of 90 degrees). On the other hand, passive tags harvest energy form the RF waves emitted by the reader antenna. With these two facts, we are inspired to estimate whether the tag is within

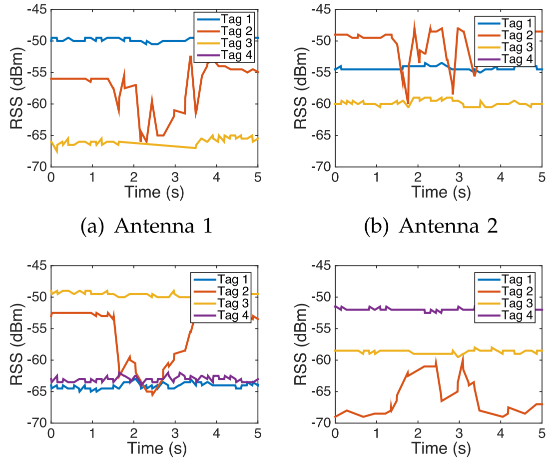

(a) Antenna 1 (b) Antenna 2

(c) Antenna 3 (d) Antenna 4

Fig. 12. RSS values of four tags under four reader antennas in the multi-user scenario.

the center monitoring region of an antenna based on its backscattered signal strength. That is, the tag with maximum RSS in a certain antenna should be the target tag. According to our experiments, within the effective range of RFID readers (around 6 m in the indoor environment), this conjecture always holds as long as there is no obstacles constantly blocking the line-of-sight between the antenna and tag.

As an illustrative measurement, we deploy four reader antennas in parallel with 1.5 m in between and ask four volunteers to stand 2 m away from the antennas. For simplicity, tag i (e.g., volunteer i, $i = 1, 2, 3, 4$) is facing antenna i, and volunteer 2 performs activities. Fig. 12 plots the RSS values of each tag collected by each antenna. In accordance with our analysis, we find that tag i has the maximum RSS in the ones collected by antenna i. In particular, in Figs. 12a and 12b, tag 4 is not even readable by antenna 1 and 2 because of its weak signal strength (e.g., lower than the minimum sensitivity of reader (say 80 dBm)). Hence, in a multi-user scenario, FEMO utilizes KL-divergence based scheme (Section 3.2.2) to find the static window before segmentation procedure, and compares the RSS of tags collected by a given antenna to determine which tag (subject) should be appropriately pairing with this antenna.

- *Interpolation-assisted Doppler profile construction.* For a COTS UHF RFID reader, all reader antennas work in a TDMA pattern. Thus, the sampling rate is decreased by a factor of M for individual tag, where M is the number of antennas in the system (M = 4 in current FEMO's implementation). To mitigate the impact of under-sampling, we study the scheduling strategy of reader antennas and find the fact that they operate in a fixed order. The working time of each antenna is short (about 0.025 s). Thus, we propose to use linear interpolation algorithm to continuously collect sufficient samples from each tag. In the implementation, we conduct interpolation on phase values and construct phased based Doppler profiles as aforementioned.

After above processes, FEMO can effectively support the multi-user exercise monitoring, just as in the single-user scenario.

3.4 Activity Assessment

The activity assessment aims to characterize the *quality* of the exercise and provides feedback to users on site. We first measure the quality for each individual activity by comparing its characteristics against the standard ones. Note that free-weight activities are often grouped where each group contains a set of repetitive activities. Activity consistency within an activity group is also essential to the gym training [24]. Hence we assess the quality of activities from two perspectives, i.e., the *local view* and *global view*, to reflect both the offset of each individual activity from the standard and the inconsistency of a activity group.

3.4.1 Local Analysis

Local analysis evaluates the quality of each activity by concentrating on its *duration* and *intensity*, which are two general criteria for evaluating the free-weight activities.

Duration. It measures how long an activity is performed by the user. The duration of an activity is critical to the free-weight training [25]. A longer duration indicates a slower arm motion, which potentially corresponds to an ineffective muscle workout. If the duration is too short, the muscle will be stretched or warped fiercely, leading to an excessive muscle workout. Either case degrades the effectiveness of gym training. In order to improve the training efficiency, FEMO measures the difference of the durations between each conducted activity and the standard. Let d_i be the duration of activity i, d_s be the duration of the corresponding standard activity. FEMO computes their difference $d_i - d_s$ and reports the result to the user at the end of each activity group.

Intensity. Intensity is another important metric to evaluate the quality of free-weight activities. It reflects the energy of the arm motions expended by an activity [26]. It is understandable that a high quality activity should show a similar energy trend to the standard. Adapting this idea to the doppler domain, it then becomes much clear that we measure the similarity between their doppler segments. Specifically, Let $A = \{a_1, a_2, \ldots, a_m\} \in \mathbb{R}^{1\times m}$ be the doppler segment of the desired activity, $B = \{b_1, b_2, \ldots, b_n\} \in \mathbb{R}^{1\times n}$ be the corresponding standard activity. In FEMO, we first align these two doppler segments by DTW to address the potential inconsistency of segment length. After that, we compute their similarity using euclidean distance metric. A shorter distance between two doppler segments indicates a higher similarity, and hence a higher performance of this activity.

3.4.2 Global Analysis

Global analysis aims at monitoring how well each group of activities are performed, with an emphasis on unveiling the abnormal activity pattern and irregular resting intervals within each activity group. This part concentrates on two kinds of characteristics: *smoothness* and *continuity*.

Smoothness. Smoothness reflects how similar each activity is to the remaining activities within an activity group. Dumbbells require more balance and more muscular control than others, such as the training with barbells or machines, and balance is crucial for optimal performance [27]. Smoothness can well reflect the balance by measuring the similarity of exercises in a group. A larger similarity indicates more regular arm actions, corresponding to effective muscle trainings. To evaluate the smoothness of an activity, we employ the discrete PDFs of all the Doppler values within an activity segment as the proposed features. Specifically, let $PDF(A) = \{p_i\}_{i=1}^{m}$ be the PDF of the activity segment A, where p_i represents the ith bin value. Since the Doppler value induced is at the granularity of 0.3 Hz, the number of bins to calculate the discrete probability distribution function is also set to the granularity of 0.3 Hz. In our measurements, we find that the fluctuation range of most Doppler values is around 6 Hz, we therefore set the number of bins to 20. To compare the similarity between two activities, we employ the Earth Mover's Distance (EMD) [28]. EMD measures the dissimilarity between two discrete probability distribution function $PDF(A) = \{p_i\}_{i=1}^{m}$ and $PDF(B) = \{q_j\}_{j=1}^{n}$. It is the minimal effort required to transform one histogram into another. Formally, the EMD between $PDF(A)$ and $PDF(B)$ is formulated as the following linear programming problem

$$
\begin{aligned}
& EMD(A,B) = \sum_{i=1}^{m}\sum_{j=1}^{n} f_{i,j}\cdot d_{i,j} \\
s.t. \quad & \sum_{i=1}^{m} f_{i,j} \le q_j, \qquad \sum_{j=1}^{n} f_{i,j} \le p_i \\
& \sum_{i,j} f_{i,j} = min\left\{\sum_i p_i, \sum_j q_j\right\}, \qquad f_{i,j} \ge 0,
\end{aligned}
$$

where $d_{i,j}$ is the ground distance between the bin i in $PDF(A)$ and the bin j in $PDF(B)$. We then calculate the EMD for each pair of activities within a group.

Continuity. Continuity depicts the consistency of resting intervals within an activity group. For efficient training, the users should pace themselves throughout the exercises [29]. A higher consistency of resting intervals indicates that the user has a good motion pace control, i.e., a regular muscle stretching/warping pace. Ideally, within an activity group, the resting intervals should be consistent with each other. However, even a professional gymnasium trainer may fail to keep strictly consistent resting intervals. Thus we model the resting interval of the standard activity group as a standard normal random variable. To evaluate the continuity of activities performed within an activity group, we investigate the statistical characteristic of resting intervals and employ kurtosis as a metric. The coefficient of kurtosis is a measurement on the degree of peakedness in a variable distribution. Specifically, let $R = \{r_i\}_{i=1}^{m}$ be the vector of resting intervals within an activity group. The kurtosis can be computed as follows:

$$
\beta_2 = \frac{\sum_{i=1}^{m}(r_i-\mu)^4}{\left(\sum_{i=1}^{m}(r_i-\mu)^2\right)^2} - 3 = \frac{\mu^4}{\sigma^4} - 3, \tag{4}
$$

where μ and δ are the mean value and standard deviation of the resting interval vector. As larger β_2 value indicates a concentrated distribution of resting intervals, therefore a better continuity of activities that the user performs.

4 System Implementation

This section presents both the hardware composition and software realization of FEMO.

Hardware. We implement a prototype of FEMO on COTS UHF RFID devices, including an ImpinJ reader Model R420, a Laird antenna model A9028R0NF (with a gain of 8 dbi), and a set of passive RFID tags. As the metal dumbbell will block the magnetic waves, we place the tag on a plastic form, which is further attached to the dumbbell. The reader is connected to a backend PC via an Ethernet cable and continuously reports the signal features backscattered from tags, including RSSIs, phase angles, and Doppler shifts. The reader connects to the host PC via Ethernet. We time-stamp each tag reading by using the reader's local clock in order to eliminate the influence of network latency.

Software. The software of FEMO is fully implemented in C#. It comprises of three components: data collection module, data analysis module and UI module. The data collection module is integrated with the Octane SDK, an extension of the LLRP Toolkit, which supports continuous tag interrogation at a rate of 340 readings/s. The data analysis module is responsible for recognizing and assessing the quality of each performed activity. The assessment results are displayed on a web-based UI module. The software runs on a Lenovo PC with an Intel Core i7-4600U 2.10 GHz CPU and 8 GB RAM.

UI Module. FEMO currently provides two services to the bodybuilder: training tracker service and activity performance assessment service. The training tracker aims to provide daily training statistics to the bodybuilder, including the accumulative training summary and daily activity summary. The former one records the training frequency, workout and duration of the bodybuilder. The latter one reports the amount of activities and average duration of each activity. In this way, FEMO provides the raw training data to the bodybuilder. The activity performance assessment service offers the quantitative performance assessment on each activity in the daily training. The user can visualize his doppler profiles of the current activity group against the standard template for evaluating his activity performance. The service also offers quantitative reports on the quality of the selected activity group against the standard template, such as the smoothness of each activity and duration/intensity differences from standard template, within each activity group. Based on the comparison, the user obtains a thorough summary on the continuity of activity groups. Although our current FEMO prototype only has fundamental functions, e.g., the visualized quality report for daily activities and logging data along the overall training process, we plan to integrate more advanced functionalities in our future work, such as the customized training reminder and intelligent training advisor.

5 System Evaluation

In this section, we conduct extensive experiments and evaluate the performance of FEMO in terms of accuracy, effectiveness, and overhead.

5.1 Experiment Setups

The experiment scenario is shown in Fig. 13. We attach two Impinj H47 passive tags on a pair of dumbbells. Each dumbbell weighs 2.5 kg. Note that the H47 passive tag is a non-metal mount tag hence does not work on metal surfaces, we thus mount it on a foam plastics that is attached on the dumbbell. The foam plastics sufficiently isolates the tag from the metal. To conduct a comprehensive evaluation, we design a training workout with the ten free-weight activities. In this workout, each activity is required to be performed with three groups of ten repetitions. Then we recruit 15 volunteers (vary in age, gender, height, and weight) to follow this workout and track their training process during two weeks. The total duration of the training is 1,534 minutes, with over 4,500 repetitions in total. The 15 volunteers are diverse in weight, height and exercise

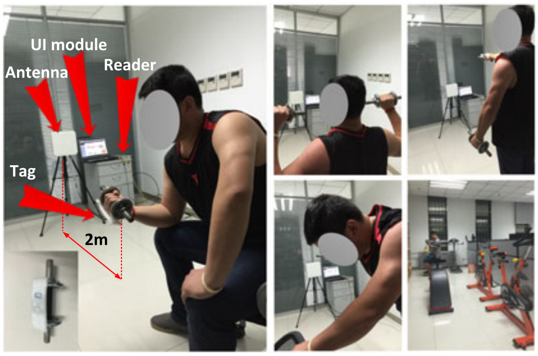

Fig. 13. Experiment scenario.

frequency. Among them, some ones are our acquaintances, and others are not. To obtain standard templates, we recruit one gym trainer who has over 5 years experience and let him perform this workout under the same settings as the other volunteers. In addition, to get the mostly effective assessment of his training, we recommend the trainer to stand at a constant place during his free-weight exercises.

5.2 Activity Segmentation

5.2.1 Evaluation Metric

We evaluate the activity segmentation scheme based on six metrics [10]: insertion rate, deletion rate, fragmentation rate, merge rate, underfill rate and accuracy. The former five metrics are used to examine the segmentation robustness while the last is to examine the overall segmentation accuracy. The detailed explanation of these metrics are as follows:

- *Insertion rate*: The proportion of cases that FEMO detects an activity within the resting interval. It examines how resilient FEMO is to noisy Doppler peaks within resting intervals.
- *Deletion rate*: The proportion of cases that FEMO misses one activity. It examines how sensitive FEMO is to weak Doppler changes incurred by gym activity.
- *Fragmentation rate*: The proportion of cases that FEMO splits a single activity into multiple ones. It evaluates the ability of FEMO in processing complicated or incoherent activities.
- *Merge rate*: The proportion of cases that FEMO merges multiple activities into a single one. It evaluates FEMO's ability in segmenting the activity with high training pace (i.e., with tiny resting intervals).
- *Underfill rate*: The proportion of cases that the segmented activity is incomplete. It examines whether our method is capable to accurately while completely excavate the entire doppler profile for an activity.
- *Accuracy*: $\frac{\#\ of\ correctly\ detected\ activity}{\#of\ activities\ that\ are\ performed}$. It examines the overall performance of FEMO on activity segmentation.

5.2.2 Evaluation Result

Fine-Grained Segmentation Performance. Fig. 14a shows the fine-grained performance of the segmentation scheme. In particular, the insertion rate is zero for activity 01 and 05. This value then increases steadily to around 0.005 for activities 02, 03, 04 and 10. Finally, it almost reaches 0.015 for activities 06, 07, and 08, which occupies ignorable portion of all the segments. For all activities, the insertion rate is extremely low. *This result indicates that our method is resilient to those doppler peaks within the resting interval.*

After checking the deletion rate, we find that it is also extremely small (below 0.01) for all the desired activities except activity 07. This is because that people usually raise the dumbbells up slowly when performing activity 07, leading to minor Doppler values. Such minor changes, in some cases, may be incorrectly put in resting intervals. Nevertheless, FEMO still controls the deletion rate below 0.02 for activity 07. *This result clearly demonstrates that FEMO is sensitive to Doppler changes incurred by the gym activity.*

As the bar chart in Fig. 14a shows, FEMO achieves diverse fragmentation rate for different activities. The fragmentation rate is relatively small for activities 02, 04, 06 and 09, i.e., below 0.01 on average. It then triples for activities 07 and 10, and further quintuples for activities 01, 03, 05 and 08. This is because activities 01, 03, 05 and 08 contain a reciprocating motion, and people tend to keep a stable posture for a while within these activities. Despite the high disparity, we observe that the overall fragmentation rate for ten activities is below 0.065. *This result shows that the probability of segmenting one activity to multiple ones is very small.*

In Fig. 14a, we also notice a gap between the maximum and minimum merge rates. This is due to the diverse training pace on different gym activities. For example, in our experiment, we find that the resting interval is relative longer for activity 01, 02 and 03, which results in a lower merge rate. While for activity 06, 08 and 09, people tend to take a short rest after performing the activity. Such a short rest leads to activity omissions, yielding a relative larger merge rate. Although the gap exists, it is still relative small (approximate to 0.05) and FEMO can achieve a merge rate of below 0.065 in the worst case. *Therefore, we can conclude that our method scales well to different training paces.*

Fig. 14a also shows the underfill rate of FEMO. We find that FEMO can precisely capture the entire Doppler profile of activity 02, 04, 06 and 09. Then the underfill rate increases slightly for more complex free-weight activities (e.g., activity 01, 03, 05 and 08). The highest underfill rate is 0.04 for activity 08, indicating FEMO can precisely capture the entire doppler profile of this activity with a success rate of 0.96. *This result clearly states that our method can accurately excavate the entire doppler profile for each activity.*

Accuracy w.r.t Activity Diversity. Fig. 14b plots the result of overall segmentation accuracy with respect to different

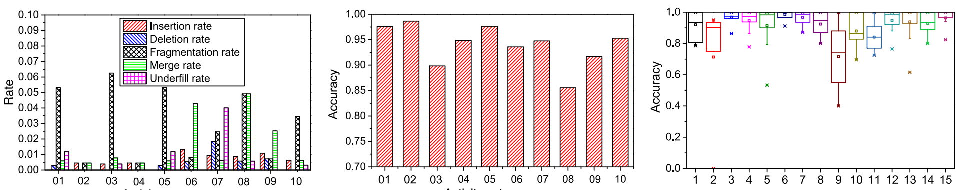

(a) Fine-grained result over 10 activities (b) Accuracy over 10 activities (c) Accuracy over 15 people

Fig. 14. Evaluation result of activity segmentation scheme.

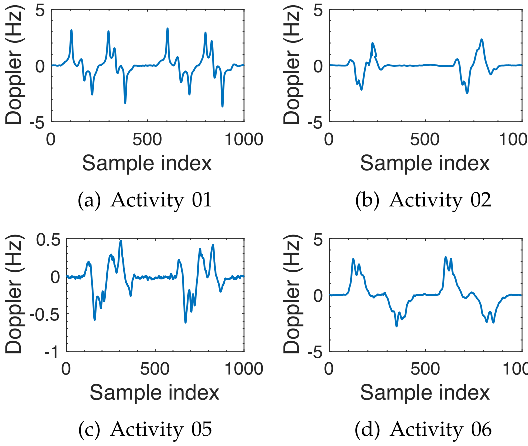

Fig. 15. Doppler profiles of activity 01, 02, 05, and 06 (two repeats in each subfigure).

activities. The performance of the segmentation result can be categorized into three groups. The first group contains activities 01, 02, 05, and 10, where FEMO achieves a segmentation accuracy over 0.95. In the second group, FEMO achieves a segmentation accuracy between 0.9 and 0.95. This group contains activities 04, 06, 07, and 09. While the last group contains activities 03 and 08. For this group, FEMO achieves an accuracy between 0.85 and 0.9. The first two categories together cover eight out of ten activities, indicating that FEMO can achieve a high accuracy (i.e., > 0.9) for the major activities. As for the last group, although the segmentation accuracy reduces, it is still above 0.85. *Therefore, we can conclude that FEMO is robust to activity diversity and can achieve desirable segmentation accuracy.*

Accuracy w.r.t Human Diversity. In this experiment, we examine the effect of human diversity on the segmentation accuracy. For each volunteer, we compute the segmentation accuracy on different activities and get the overall accuracy distribution. The result is shown in Fig. 14c. The overall segmentation accuracy for the 15 volunteers maintains in a high level. Specifically, the median accuracy is above 0.9 for 12 volunteers. For the remaining 3 volunteers (volunteer 9, 10, and 11), we can see that FEMO achieves a relative inferior performance, with an accuracy of 0.83 on average. Interestingly, based on the physical characteristic records of volunteers, we find that all the three volunteers seldom go to the gym. As a result, the lack of exercise of these volunteers may lead to non-standard behaviors, thus lowering the segmentation accuracy of FEMO. We further investigate the fine-grained segmentation accuracy distribution of each volunteer. We can see that as shown in Fig. 14c, those who take exercise regularly (e.g., volunteer 3, 4, 6 and 12), the box is relatively short, suggesting that the segmentation accuracy of overall activities has a high level similarity with each other. While for those sedentary group (e.g., volunteer 9, 10 and 11), we can see that the box of accuracy distribution is comparatively tall, indicating that FEMO holds different accuracy performance on different kinds of activities.

5.3 Evaluation on Activity Recognition

5.3.1 Evaluation Metric

It is possible that the activity recognition system can miss, confuse, or falsely detect activities that did not occur. Thus, in evaluating our activity recognition scheme, we employ the following three metrics:

Actual label	Predicted label									
	A 01	A 02	A 03	A 04	A 05	A 06	A 07	A 08	A 09	A 10
A 01	0.89	0.03	0	0	0.03	0.05	0	0	0	0
A 02	0.01	0.89	0	0	0.05	0.05	0	0	0	0
A 03	0	0	0.88	0	0	0	0.07	0.04	0	0.01
A 04	0	0	0	0.93	0	0	0	0	0.07	0
A 05	0.02	0.02	0	0	0.94	0.02	0	0	0	0
A 06	0.06	0.02	0	0	0.03	0.90	0	0	0	0
A 07	0	0	0.04	0	0	0	0.89	0.03	0	0.04
A 08	0	0	0.03	0	0	0	0.03	0.93	0	0.01
A 09	0	0	0	0.16	0	0	0	0	0.84	0
A 10	0	0	0.01	0	0	0	0.02	0.02	0	0.95

Fig. 16. Confusion matrix of activity recognition.

Precision P. $\frac{TP}{TP+FP}$, where TP and FP represent the true positives and the false positives. Precision is the fraction of correctly recognized activities that are relevant to all the recognized activities.

Recall R. $\frac{TP}{TP+FN}$, where FN is the false negatives. Recall is the fraction of the correctly recognized activities that are relevant to all this kind of activities.

False Positive Rate FPR. The proportion of cases that FEMO mistakes an activity for other activities.

5.3.2 Evaluation Result

Overall Accuracy on Different Activities. Note that when conducting the activity recognition, we only compare the profile of current activity against the templates in the sub-class (i.e., one-arm, in parallel, or alternative). Fig. 15 shows the actual measurements (i.e., Doppler profile) of activity 01, 02, 05, and 06 that all belong to the one-arm sub-class. The results indicate that the profile is distinguishable. Detailed profiles of other activities are skipped due to space limit. Instead, we show recognition accuracy for all activities using the fusion matrix in Fig. 16. The data is collected from 15 volunteers. In Fig. 16, each row denotes the actual activity performed and each column represents the activity recognized by FEMO. Each element in the matrix represents the fraction of activities in the row that were regarded as the activity in the column. As is shown, the average accuracy is 0.90 with a standard deviation of 0.03 for 10 gym activities. This shows that we can extract rich information about free-weight activities from the Doppler profiles. *The result clearly shows that FEMO achieves a high and stable activity recognition performance, due to its efficient Doppler profile extraction scheme and robust profile matching algorithm.*

Examine the Fine-Grained Performance. In this experiment, we examine the the precision, recall and false positive rate of the recognition performance. The result is shown in Fig. 17. FEMO achieves an average precision of 0.90 with a standard deviation of 0.04. This result demonstrates that FEMO substantially returns more actual labels to the activity than error labels. As Fig. 17 shows, although the recall fluctuates over different activities, it still maintains a high level for all of these 10 activities, achieving a mean value of 0.91 with a standard deviation of 0.03. This result demonstrates that FEMO can recognize all of these 10 activities with high accuracy. *In a nutshell, the high precision and recall achieved by FEMO manifests that our recognition scheme scales well to different activities.*

We then examine the FPR of the recognition result. A higher FPR implies a great portion of other activities that are mistakenly classified as the targeting activity. As a result, people may ignore the system's notifications and

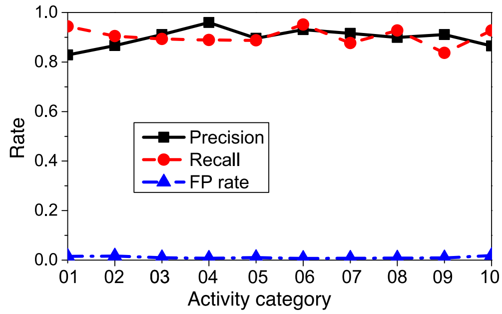

Fig. 17. Precision, recall, and FP.

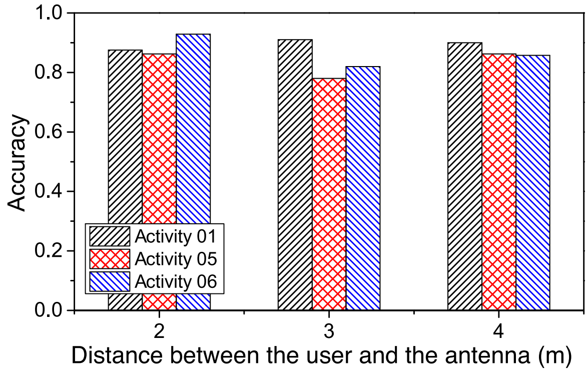

Fig. 18. Accuracy over different antenna-to-user distances.

eventually abandon the system. Fig. 17 shows the *FPR* cross 10 activities. We observe that FEMO achieves an average FP rate of 0.011 with a standard deviation of 0.004. Such a low FP rate suggests that FEMO rarely takes other activities as the targeted activity. Therefore, we can trust the activity recognition result with high confidence.

Impact of Antenna-to-User Distance. We further examine the impact of antenna-to-user distance on the activity recognition. In this trail of experiments, we ask three volunteers to perform activities under different antenna-to-user distance settings. Each activity is performed 30 times by each volunteer. For each activity, we average the recognition accuracy of these volunteers. We randomly pick out three activities and show their recognition accuracy in Fig. 18. As the result indicates, when the user is with close proximity to the antenna, the recognition accuracy of these three activities all maintain in a high level. As we expand the user-to-antenna distance, the recognition accuracy changes moderately. *This result clearly demonstrates that our recognition scheme is insensitive to the user-to-antenna distance*.

Impact of Angle. In this part, we test how the orientation of the subject to the reader impacts the recognition accuracy. In these experiments, a volunteer stands at different places along a line which is 2 m away from the center of reader antenna to form different angles (0 degree is the default setting in FEMO), as shown in Fig. 19a. Three activities (activity 01, 05, and 06) are performed, each for 30 times. The average recognition accuracy is reported in Fig. 19b. The results indicate that as the angle gets larger, the accuracy decreases gradually. Specifically, when the angle is 30 degree, FEMO can still achieve an accuracy of almost 90 percent. But when the angle is 60 degree, the accuracy decreases by 20 percent. Based on our experimental result, we recommend the users to directly face the antenna when performing activities (or arrange the layout of the fitness region to meet this requirement).

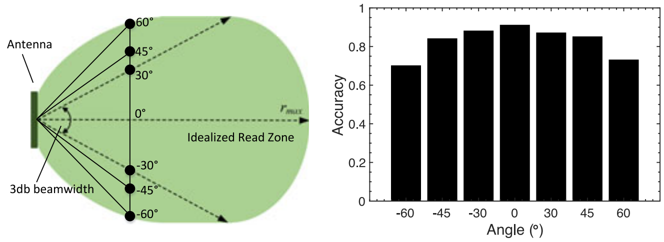

(a) Experimental setups (b) Recognition accuracy

Fig. 19. Recognition accuracy over different angles.

5.4 Evaluation on Activity Assessment

FEMO can show the user the detailed assessment information about *Duration*, *Intensity*, *Smoothness*, and *Continuity* of his/her exercises. Then, to evaluate the activity assessment service, we survey the 15 volunteers to get qualitative feedback on the effectiveness and practicability of our system objectively based on their true experience. This includes the user satisfaction and attractive feature. For each aspect, the volunteer is required to give a score between 1 (lowest) to 5 (highest). And we treat these scores as the evaluation for our activity assessment module.

Overall Feedbacks. Table 1 shows the overall feedback on FEMO. Participants consider that FEMO could help to reach the training goal with an average satisfaction score of 4.5, the standard deviation is 0.6. The potential to motivate regular training achieves a score of 4.7 on average, with std=0.4. Besides, participates also show high interest (4.6) to use FEMO for monitoring their free-weight training process. Overall, the feedback confirms that FEMO can help to reach training goals faster, motivate the training, and attract participants for long-term use.

Attractive Services. Table 2 shows the ratings on different services provided by FEMO. In the result, the most attractive services that the participants agree with is the accumulative training summary and the local assessment. These two services are scored 4.7. The global assessment is also attractive, achieving a score of 4.6. Although the daily activity summary is less attractive compared with the others, it still achieves a pretty high score (4.3 with std=0.4). Therefore, from above results we believe that FEMO really provides valuable feedback to the user.

6 Rear-World Deployment

We deploy our FEMO system into a small fitness room in our lab. As the bottom-right figure shown in Fig. 13, there are other equipments coexisting, such as treadmills and pedalling machines. We conduct experiments in this scenario and test the robustness of FEMO under different scenarios.

6.1 Impact of Surroundings

In this trail of experiments, we ask three volunteers to perform activities under various conditions. The first group of experiments (Condition #1) are conducted in normal environments, e.g., relatively constant surroundings. In the second group of experiments (Condition #2), the volunteers still perform their dumbbell activities. However, we introduce certain dynamics to the environment by allowing some other trainers to run on the treadmills concurrently, indicating that the environment is dynamic compared with Condition #1. During the third group of experiments (Condition #3), a disturber walks across the line of sight between

TABLE 1
Feedback on FEMO After Two Weeks Training

Feedback item	Rating	std
could help to reach the training goal	4.5	0.6
could help to rectify the irregular motion	4.7	0.4
would continue using it	4.6	0.6

TABLE 2
Service Assessment After Two Weeks Training

Service item	Rating	std
accumulative training summary	4.7	0.3
daily activity summary	4.3	0.4
global assessment	4.6	0.5
local assessment	4.7	0.4

the reader antenna and the volunteer frequently to simulate the impact from other trainers in real-world scenarios. Every volunteer performs each activity 50 times under each condition. The segmentation and the recognition accuracy are shown in Figs. 20 and 21. From the results we can see that the segmentation accuracy scales well across three conditions. In particular, both the segmentation and recognition accuracy (say 0.92 and 0.87) under condition #2 are slightly influenced, which is supportive for FEMO robustness in real deployments. We notice that the recognition accuracy has a significant reduction under condition #3. It proves that when the line of sight from the reader antenna to the user is frequently blocked, the Doppler profile will change sharply and hence be hardly recognized. This indicates us that we need to avoid such events by carefully arranging the site layout in real deployments. On the other hand, if the reader's antenna is deployed on the ceiling, the probability that such a case occurs is extremely low. Thus, we can safely argue that environmental impact to the deployment of FEMO in a real gym would be negligible.

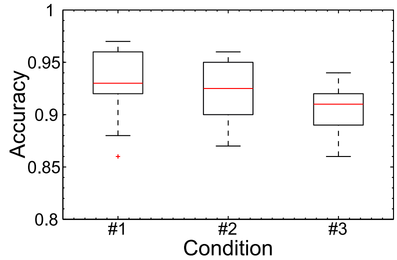

Fig. 20. Segmentation accuracy over various conditions.

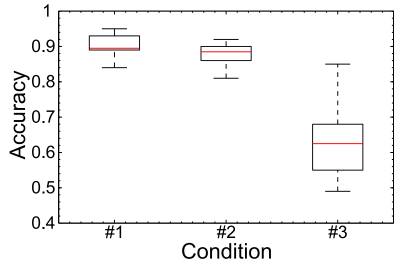

Fig. 21. Recognition accuracy over various conditions.

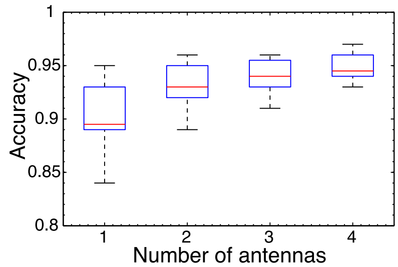

Fig. 22. Impact of different number of antennas.

6.2 Multi-Antenna Scenario

We vary the number of reader antennas used for monitoring one trainer and observe the activity recognition accuracy. In this experiment, the volunteer performs activities with two, three, and four antennas coexisting respectively. The antennas are placed parallel to each other with panels directly facing the volunteer. The distance between the antenna and the volunteer is 2 m. Fig. 22 depicts the relationship between the number of antennas and the recognition accuracy. The accuracy is about 91 percent on average when adopting one antenna. With more antennas, the average recognition accuracy of FEMO improves gradually and achieves about 94 percent when the number of antennas is four. In addition, the gap of accuracy between each activity becomes narrower. The reason lies in that more antennas can provide multi-dimensional feature for each activity, which can complement with each other. Moreover, the result proves that using more antennas can further improve FEMO's efficiency.

6.3 Multi-User Scenario

We also test the accuracy of FEMO in the multiple-user scenario. In this trail of experiments, we ask multiple volunteers to perform activities concurrently. We conduct two groups of experiments. In the first group, only one antenna is adopted for monitoring, and the antenna is 2 m away from the volunteers. In this case, when there are more than one user, different users (e.g., tags) may have different angles to the reader antenna. In the second group, we deploy multiple antennas and each antenna is responsible to monitor one volunteer (e.g., each volunteer stands facing one antenna). Fig. 23 shows the recognition accuracy versus different number of volunteers. As expected, if increasing the number of trainers, the accuracy decreases accordingly when using a single antenna. This is because the angle between the reader and tag leads changes to Doppler profiles, which further introduces ambiguity to the system. In particular, when the number of volunteers is four, the accuracy decreases sharply, i.e., around to 85 percent. On the contrary, when adopting multiple antennas, the recognition accuracy of FEMO can always maintain in a high level (say 90 percent) even with multiple users.

7 Related Work

The design of FEMO is closely related to the activity recognition technique. There is a large body of works on human activity recognition. Based on different processing patterns, the works in this domain can be broadly divided into two categories. The first category of works leverage dedicated sensors [4], [22], [37], e.g., the gyroscope and accelerometer, for human activity recognition. These works build upon the fact that the sensor can provide rich information reflecting the gesture recognition. UbiFit Garden [4] infers the body movement via a on-body sensing module, and displays the result on the mobile terminal to encourage individuals' training

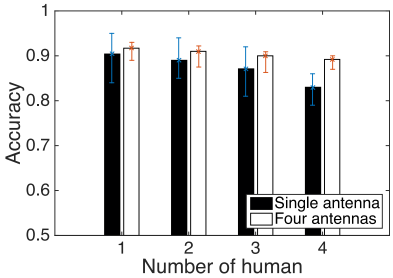

Fig. 23. Impact of multiple human.

enthusiasm. RistQ [22] leverages the accelerations from a wrist strap to detect and recognize smoking gestures. Chang et al. [12] also use accelerometer sensors embedded in a glove to recognize and track the free-weight exercises in the gym. Although these proposals have demonstrated an inspiring power in activity recognition, the requirement of wearing some dedicated sensors is usually cumbersome or unsuitable for gym activity recognition. Besides, the performance of these sensor based schemes is sensitive to the hardware characteristics (e.g., the sampling rate or computational capacity), which limits the wide adoption in practice.

Another brunch of solutions exploits the wireless signals. A lot of efforts have been made to improve the efficiency of wireless networks [38], [39], [40], [41], [42], providing the feasibility of utilizing wireless signals for gesture and activity recognition. RF-IDraw [30] can infer a human's writing by tracking a passive RFID tag attached to his/her pen. E-eyes [16] leverages WiFi signals to recognize the in-home activity of human beings. In particular, there are many prior works detecting movements by resorting to Doppler effect [31], [32], [33], [34], [35]. Their common insight is that the Doppler shift generated from the non-rigid-body motions of humans contains valuable information related to the human movement. The authors in [31], [33] extract certain features from the Doppler shift to distinguish among humans, animals, and vehicles. The work proposed in [32] can classify seven human activities (such as the running, walking, etc.) by extracting Doppler features from the signals collected by a 2.4 GHz Doppler radar. WiSee [15] exploits the Doppler effect of WiFi signals caused by the body reflection to infer nine typical human motions. Similar to our work, these approaches are device-free such that users are released from wearing or carrying any devices. However, they either adopt dedicated hardware (e.g., Software defined radio, Doppler radar, etc.) or require complicated signal processing procedure, introducing a high deployment cost or huge computational overhead. Moreover, they have to rely on high-frequency signals (such as 2.4 GHz, 24 GHz), in which cases the Doppler change induced by human motions are obvious and easy to track. Our work releases this constraint in that we realize the accurate activity recognition and assessment by using a much lower frequency spectrum, i.e., 860 MHz $\sim$ 960 MHz, which is adopted by COTS passive RFID devices. Within this spectrum, the Doppler changes are subtle and vulnerable to noises [36]. In addition, we enable the on-site activity recognition and assessment by adopting several efficient techniques, e.g., DTW, and provide rich feedbacks to the user for assessments.

8 Conclusion

In this paper, we present the design, implementation and evaluation of FEMO, a passive RFID based free-weight activity monitoring system. FEMO attaches passive RFID tags to the training devices, i.e., dumbbell in this work, and leverages the backscattered signal for on-site activity recognition and assessment. The result of extensive experiments collected from 15 volunteers demonstrates that FEMO can be applied to a variety of free-weight activities, providing valuable feedbacks for users' activity rectification.

Acknowledgments

This work was supported by National Basic Research Program of China (973 Program) under Grant No. 2015CB351705, NSFC Grant No. 61572396, 61373175, 61402359, 61325013, China 863 Grant 2013AA014601, and National Science and Technology Major Project of the Ministry of Science and Technology of China JZ-20150910. Panlong Yang is supported by NSF of Jiangsu for Distinguished Young Scientist: BK20150030, NSFC with No. 61632010. Longfei Shangguan is the corresponding author.

References

[1] J. Kruger, H. M. Blanck, and C. Gillespie, "Dietary and physical activity behaviors among adults successful at weight loss maintenance," *Int. J. Behavioral Nutrition Phys. Activity*, vol. 3, no. 1, 2006, Art. no. 17.
[2] Centers for disease control and prevention. Physical activity recommendations for adults. (2015). [Online]. Available: cdc.gov/physicalactivity/everyone/guidelines/adults.html
[3] Free-weight exercises. (2015). [Online]. Available: http://www.building-muscle101.com/
[4] S. Consolvo, et al., "Activity sensing in the wild: A field trial of Ubifit garden," in *Proc. SIGCHI Conf. Human Factors Comput. Syst.*, 2008, pp. 1797–1806.
[5] S. B. Eisenman, E. Miluzzo, N. D. Lane, R. A. Peterson, G.-S. Ahn, and A. T. Campbell, "BikeNet: A mobile sensing system for cyclist experience mapping," *ACM Trans. Sensor Netw.*, vol. 6, no. 1, 2009, Art. no. 6.
[6] Fitbit. (2017). [Online]. Available: https://www.fitbit.com/
[7] iOS 8 HealthKit. (2017). [Online]. Available: http://www.apple.com/ios/whats-new/health/
[8] A. Zhan, M. Chang, Y. Chen, and A. Terzis, "Accurate caloric expenditure of bicyclists using cellphones," in *Proc. 10th ACM Conf. Embedded Netw. Sensor Syst.*, 2012, pp. 71–84.
[9] Are personal trainers worth the price. (2011). [Online]. Available: http://www.telegraph.co.uk/health/dietandfitness.html
[10] A. Bulling, U. Blanke, and B. Schiele, "A tutorial on human activity recognition using body-worn inertial sensors," *ACM Comput. Surveys*, vol. 46, no. 3, 2014, Art. no. 33.
[11] H. Lu, J. Yang, Z. Liu, N. D. Lane, T. Choudhury, and A. T. Campbell, "The Jigsaw continuous sensing engine for mobile phone applications," in *Proc. 8th ACM Conf. Embedded Netw. Sensor Syst.*, 2010, pp. 71–84.
[12] K.-H. Chang, M. Y. Chen, and J. Canny, "Tracking free-weight exercises," in *Proc. 9th Int. Conf. Ubiquitous Comput.*, 2007, pp. 19–37.
[13] D. Morris, T. S. Saponas, A. Guillory, and I. Kelner, "RecoFit: Using a wearable sensor to find, recognize, and count repetitive exercises," in *Proc. SIGCHI Conf. Human Factors Comput. Syst.*, 2014, pp. 3225–3234.
[14] P. Melgarejo, X. Zhang, P. Ramanathan, and D. Chu, "Leveraging directional antenna capabilities for fine-grained gesture recognition," in *Proc. ACM Int. Joint Conf. Pervasive Ubiquitous Comput.*, 2014, pp. 541–551.
[15] Q. Pu, S. Gupta, S. Gollakota, and S. Patel, "Whole-home gesture recognition using wireless signals," in *Proc. 19th Annu. Int. Conf. Mobile Comput. Netw.*, 2013, pp. 27–38.
[16] Y. Wang, J. Liu, Y. Chen, M. Gruteser, J. Yang, and H. Liu, "E-eyes: Device-free location-oriented activity identification using fine-grained WiFi signatures," in *Proc. 20th Annu. Int. Conf. Mobile Comput. Netw.*, 2014, pp. 617–628.
[17] N. Y. Hammerla, T. Plötz, P. Andras, and P. Olivier, "Assessing motor performance with PCA," in *Proc. Int. Workshop Frontiers Activity Recognit. Pervasive Sensing*, 2011, pp. 18–23.

[18] R. E. Kalman, "A new approach to linear filtering and prediction problems," *J. Fluids Eng.*, vol. 82, no. 1, pp. 35–45, 1960.
[19] Impinj, "Speedway revolution reader application note-low level user data support," Impinj, Seattle, WA, USA, 2013.
[20] L. G. Roberts, "ALOHA packet system with and without slots and capture," *ACM SIGCOMM Comput. Communn. Rev.*, vol. 5, no. 2, pp. 28–42, 1975.
[21] R. A. Leibler and S. Kullback, "On information and sufficiency," *Ann. Math. Statist.*, vol. 22, pp. 79–86, 1951.
[22] A. Parate, M.-C. Chiu, C. Chadowitz, D. Ganesan, and E. Kalogerakis, "RisQ: Recognizing smoking gestures with inertial sensors on a wristband," in *Proc. 12th Annu. Int. Conf. Mobile Syst. Appl. Services*, 2014, pp. 149–161.
[23] S. Salvador and P. Chan, "Toward accurate dynamic time warping in linear time and space," *Intell. Data Anal.*, vol. 11, no. 5, pp. 561–580, 2007.
[24] C. Kennedy-Armbruster and M. Yoke, *Methods of Group Exercise Instruction*. Champaign, IL, USA: Human Kinetics, 2014.
[25] Learn how to slim and strengthen your midsection with the best core exercises. (2008). [Online]. Available: http://www.askthetrainer.com/best-core-exercises/
[26] How to measure exercise intensity. (2017). [Online]. Available: http://www.weightwatchers.com/util/art/index_art.aspx?tabnum=1&art_id=20971
[27] Dumbbells, barbells, and kettlebells. (2011). [Online]. Available: http://www.bodybuilding.com/fun/grapgym9.htm
[28] Y. Rubner, C. Tomasi, and L. J. Guibas, "The earth mover's distance as a metric for image retrieval," *Int. J. Comput. Vis.*, vol. 40, no. 2, pp. 99–121, 2000.
[29] A simple protocol for testing your work capacity. (2014). [Online]. Available: http://breakingmuscle.com/strength-conditioning/a-simple-protocol-for-testing-your-work-capacity
[30] J. Wang, D. Vasisht, and D. Katabi, "RF-IDraw: Virtual touch screen in the air using RF signals," in *Proc. ACM Conf. SIGCOMM*, 2014, pp. 235–246.
[31] I. Bilik, J. Tabrikian, and A. Cohen, "GMM-based target classification for ground surveillance Doppler radar," *IEEE Trans. Aerospace Electron. Syst.*, vol. 42, no. 1, pp. 267–278, Jan. 2006.
[32] Y. Kim and H. Ling, "Human activity classification based on micro-Doppler signatures using a support vector machine," *IEEE Trans. Geoscience Remote Sens.*, vol. 47, no. 5, pp. 1328–1337, May 2009.
[33] A. Stove and S. Sykes, "A Doppler-based automatic target classifier for a battlefield surveillance radar," in *Proc. IEEE RADAR*, 2002, pp. 419–423.
[34] D. A. Tesch, E. L. Berz, and F. P. Hessel, "RFID indoor localization based on Doppler effect," in *Proc. 16th Int. Symp. Qual. Electron. Des.*, 2015, pp. 556–560.
[35] S. Masatoshi and M. Kurato, "Activity recognition using radio Doppler effect for human monitoring service," *J. Inf. Process.*, vol. 20, no. 2, pp. 396–405, 2012.
[36] H. Li, Y. Can, and P. S. Alanson, "IDSense: A human object interaction detection system based on passive UHF RFID," in *Proc. 33rd Annu. ACM Conf. Human Factors Comput. Syst.*, 2015, pp. 2555–2564.
[37] P. Zhou, Y. Zheng, Z. Li, M. Li, and G. Shen, "Iodetector: A generic service for indoor outdoor detection," in *Proc. ACM SenSys*, 2012.
[38] K. Wu, H. Li, L. Wang, Y. Yi, Y. Liu, D. Chen, X. Luo, Q. Zhang, and L. M. Ni, "hJam: Attachment transmission in WLANs," *IEEE Trans. Mobile Comput.*, vol. 12, no. 12, pp. 2334–2345, 2013.
[39] J. Wang, S. Lian, W. Dong, X.-Y. Li, and Y. Liu, "Every packet counts: Loss and reordering identification and its application in delay measurement," *IEEE/ACM Trans. Netw.*, vol. 24, no. 6, pp. 3426–3438, 2016.
[40] G. Wang, S. Zhang, K. Wu, Q. Zhang, and L. M. Ni, "TiM: Fine-grained rate adaptation in WLANs," *IEEE Trans. Mobile Comput.*, vol. 15, no. 3, pp. 748–761, 2016.
[41] X. Ji, Y. He, J. Wang, K. Wu, D. Liu, K. Yi, and Y. Liu, "On improving wireless channel utilization: A collision tolerance-based approach," *IEEE Trans. Mobile Comput.*, vol. 16, no. 3, pp. 787–800, 2017.
[42] H. Li, K. Wu, Q. Zhang, and L. M. Ni, "CUTS: Improving channel utilization in both time and spatial domain in WLANs," *IEEE Trans. Parallel Distrib. Syst.*, vol. 25, no. 6, pp. 1413–1423, 2014.

Han Ding received the BS degree in software engineering from Xi'an Jiaotong University, in 2011. She is currently working toward the PhD degree at Xi'an Jiaotong University. Her research interests focus on indoor localization, smart sensing, and RFID systems. She is a student member of the IEEE.

Jinsong Han received the PhD degree in computer science from the Hong Kong University of Science and Technology, in 2007. His research interests focus on mobile computing, RFID, and wireless network. He is a senior member of the ACM and the IEEE.

Longfei Shangguan received the BS degree in software engineering from Xidian University, in 2011 and the PhD degree from HKUST, in 2015. He is currently a postdoc research associate in the Computer Science Department, Princeton University. His research interests include indoor localization and RFID system. He is a student member of the IEEE and the ACM.

Wei Xi received the PhD degree in computer science computer science and technology from Xi'an Jiaotong University, in 2014. His research interests focus on wireless networks, smart sensing, and mobile computing. He is a member of the CCF, the ACM, and the IEEE.

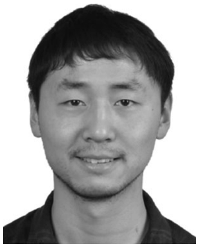

Zhiping Jiang is currently working toward the PhD degree at Xi'an Jiaotong University. His research interests focus on localization, smart sensing, wireless communication, and image processing. He is a student member of the IEEE.

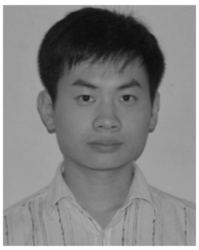

Zheng Yang received the BS degree in computer science from Tsinghua University and the PhD degree from HKUST. He is currently an assistant professor in the School of Software and TNList, Tsinghua University. His research interests focus on wireless networking, mobile computing, pervasive computing, and sensor networks. He is a member of the IEEE and the ACM.

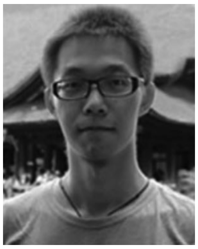

Zimu Zhou received the BS degree in electronic engineering from Tsinghua University, in 2011 and the PhD degree from HKUST, in 2015. He is currently a post-doctoral researcher in the Computer Engineering Group, ETH Zurich. His research interests include wireless networks, ubiqutious computing, and RFID systems. He is a student member of the IEEE.

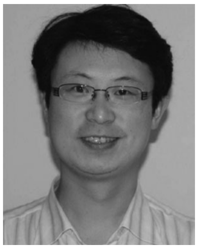

Panlong Yang received the PhD degree in communication and information system from the Nanjing Institute of Communication Engineering, in 2005. He was a visiting scholar with HKUST during September 2010 to September 2011. He is an associate professor in the Nanjing Institute of Communication Engineering, PLA University of Science and Technology. His research interests focus on mobile communication, wireless network, wireless sensor network, and social network analysis. He is a member of the IEEE Computer Society and the ACM SIGMOBILE Society.

Jizhong Zhao received the PhD degree in computer science and technology from Xi'an Jiaotong University, in 2001. His research interests focus on computer software, pervasive computing, distributed systems, and network security. He is a member of the CCF, the ACM, and the IEEE.